Numerical simulations of neoclassical transport in the pedestal region of a tokamak plasma

A. Bergmann[1], S. D. Pinches[2], E. Wolfrum[1]

[1] *Max-Planck-Institut für Plasmaphysik, IPP–EURATOM Association, 85748 Garching, Germany*

[2] *EURATOM/CCFE Fusion Association, Culham Science Centre, Abingdon, Oxfordshire, OX13 6PR, UK*

At the edge of a high-confinement mode (H-mode) plasma in present large tokamaks a narrow region (pedestal) with large density and temperature gradients exists. The width of this region and the scale length of the radial variations of density and temperature is of order of the poloidal ion gyro radius [1], such that a basic scaling assumption of the standard neoclassical theory [2] is violated. Furthermore, in the pedestal a strong electric field is present that varies on the same length scale. A large gradient of the electric field can lead to squeezing or widening of the banana orbits [3] which effects the neoclassical transport [4, 5]. Recently, a new theory for these conditions was presented [6], which includes the effect of a strong electric field with $E_r/B_p \approx v_{\mathrm{thi}}$. In both theories the large aspect ratio limit is assumed for obtaining analytical expressions, neglecting terms of order $\sqrt{\varepsilon}$.

Here, we study neoclassical physics in the plasma edge with guiding-centre particle simulations, which intrinsically include the effects due to the deviation of the particle orbits from the flux surfaces and thus capture possible effects of reduced or increased orbit size. For given radial profiles of density, temperature and electric potential the distribution functions of ions and electrons are obtained. The delta-f code HAGIS [7] with a Monte Carlo model of Coulomb collisions [8] is used. The deviation of the distribution function from a Maxwellian is represented by marker particles, the motion of which is described by guiding-centre equations derived from a Lagrangian. Pitch-angle scattering with the velocity dependent Coulomb collision frequency is applied and a correction term is added to the particle weights to ensure momentum conservation. In the calculations for the ions the ion-electron collisions can be neglected, since the momentum loss caused by them is very small. For obtaining the bootstrap current, simulations for the electrons are performed including the collisions with the ions, where the ion distribution function is approximated by a shifted Maxwellian [8].

The large pressure gradient in the pedestal would cause a fast toroidal plasma rotation if it was not balanced by a strong radial electric field just where the pressure gradient is large. This electric field almost cancels the contribution of the pressure gradient to the toroidal velocity, which usually has a minimum in the pedestal. Typically the pedestal plasma is in the banana-

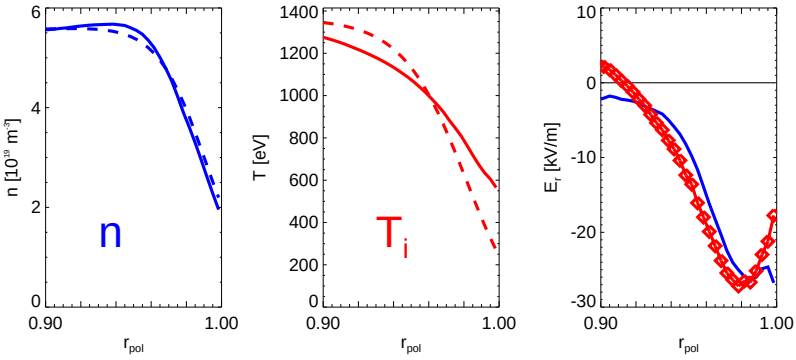

Fig. 1: Profiles of density and temperature (dashed: initial), and electric field (red) and $\nabla p/en$ (blue) for case I. $r_{\rm pol} = \sqrt{\psi/\psi_{\rm a}}$.

plateau transition or plateau regime ($0.1 < \nu^* < \varepsilon^{-3/2}$, $\nu^* = \nu q R_0/\varepsilon^{3/2} v_{\rm thi}$) and the trapped particle fraction is $f_t \approx 0.7$. Hence, the coefficient k_i in the expression for the poloidal flow, $u_p = -k_i (RB_t B_p)/(e\langle B^2\rangle) dT_i/d\psi$, is small [9]. Here, ψ is the poloidal flux, B_t and B_p are toroidal and poloidal magnetic field and the angular brackets denote the flux surface average. In Fig. 2 the numerical results for the parallel and poloidal velocities are shown for a case with moderately steep profiles (case I, see Fig. 1, the evolution of n and T is also shown). Where the gradients are large, the poloidal velocity differs from the standard theory ([9], for finite ε) and a corresponding deviation is seen in the parallel velocity. A large gradient of the electric field can lead to squeezing or widening of the banana orbits, The ratio $S = w_0/w$ is $S = 1 + \alpha$ for large aspect ratio with $\alpha = (RB_t)^2 d^2\Phi/d\psi^2/B\Omega \approx -\rho_{\rm pol}(dE_r/dr)/B_p v_{\rm thi}$ [3], where $\rho_{\rm pol} = v_{\rm thi}/\Omega_p$, $v_{\rm thi} = \sqrt{2T_i/m_i}$ and Ω_p is the cyclotron frequency calculated with B_p. The parameter α is the second order coefficient in a local expansion of the electric potential,

$$e\Delta\Phi/T_i = -2(u/v_{\rm thi})(\Delta r/\rho_{\rm pol}) + \alpha\,(\Delta r/\rho_{\rm pol})^2 + \gamma\,(\Delta r/\rho_{\rm pol})^3 + \delta\,(\Delta r/\rho_{\rm pol})^4 + \ldots \qquad (1)$$

with $u = E_r/B_p$, $\gamma = (v_{\rm thi}/3)(RB_t)^3 d^3\Phi/d\psi^3/B\Omega^2$ and $\delta = (v_{\rm thi}^2/12)(RB_t)^4 d^4\Phi/d\psi^4/B\Omega^3$. At large aspect ratio orbit squeezing does not affect the parallel or poloidal velocity [4], but a strong electric field does modify the poloidal velocity according to [6]. In case I this theory is very close to the blue line in Fig. 2, since the parameter $|u/v_{\rm thi}|$ is rather small. In Fig. 3 $u/v_{\rm thi}$

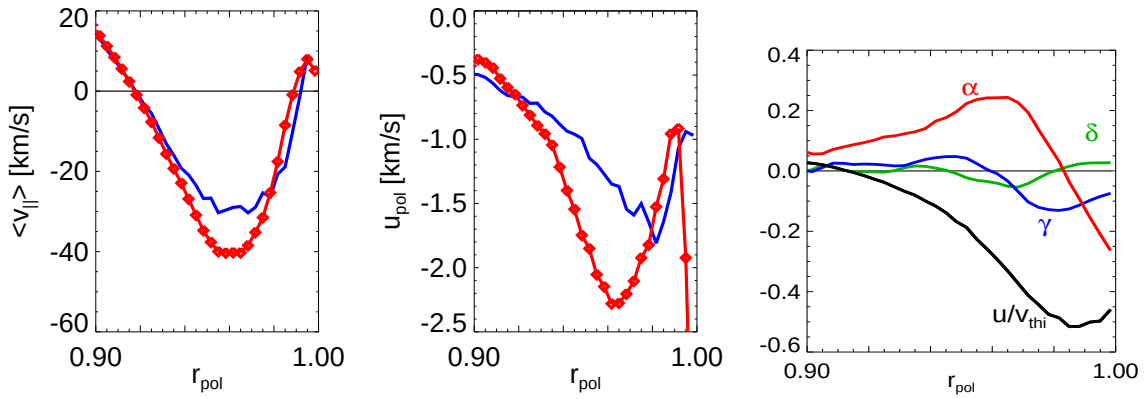

Fig. 2: Parallel velocity (left) and poloidal velocity (centre) compared with (blue) theory [9].
Fig. 3 (right): $u/v_{\rm thi} = (E_r/B_p)/v_{\rm thi}$ and coefficients α, γ and δ of electric potential, Eq.(1).

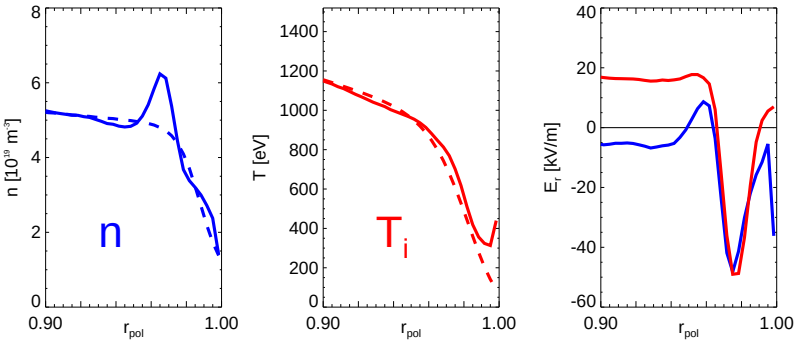

Fig. 4: Profiles of density and temperature (dashed: initial), and electric field (red) and $\nabla p/en$ (blue) for case II. $r_{\rm pol} = \sqrt{\psi/\psi_{\rm a}}$.

is shown together with the coefficients α, γ and δ. In Figs. 5–7 results for case II with larger gradients are depicted, the density and temperature profiles and the electric field are shown in Fig. 4. Here, the peak value of $|u|$ is close to the thermal speed and $|\alpha|_{\rm max}$ exceeds unity (Fig. 5a). The deviation of the poloidal velocity (Fig. 5b) from the theory [9] (new theory [6] is shown by a dashed line) is much larger than in the first case, resulting in a sheared flow. There is a corresponding change of the parallel velocity (Fig. 6), but the relative change is smaller for the parallel ion current in the frame rotating with the velocity $u = E_r/B_p$ (Fig. 7), since $|u| \gg \langle v_\parallel \rangle_{\rm Labframe}$ holds around the peak of E_r. This current affects the ion contribution to the bootstrap current, which is shown in Fig. 8. In the case I the numerical result is close to the standard theory, whereas in the case II with larger gradients there is a small deviation as a consequence of the changed ion current shown in Fig. 7.

The radial heat flux is compared in Fig. 9 with the expressions from [5] (solid) with a factor $(1+\alpha)^{-3/2}$ and from [6] with a factor $(1+\alpha)^{1/2}$ multiplied by a function of $(u/v_{\rm thi})^2$ (dashed). Where orbits are squeezed ($\alpha > 0$), the heat flux is closer to theory [5]. When E_r is large, energy scattering, which is neglected in the simulations, also contributes to scattering

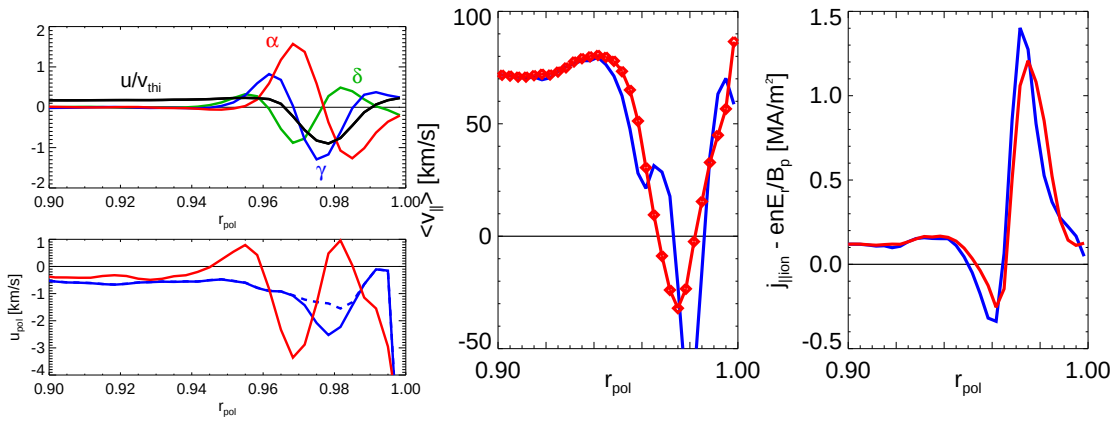

Fig. 5: **top**: Coefficients of electric potential, Eq. (1); **bottom**: poloidal velocity (red) compared with theory (blue, solid: [9], dashed: [6]). **Fig. 6**: Parallel velocity (red) compared with theory [9] (blue). **Fig. 7**: Parallel ion current (red) in the frame rotating with $u = E_r/B_p$. Blue: theory [9].

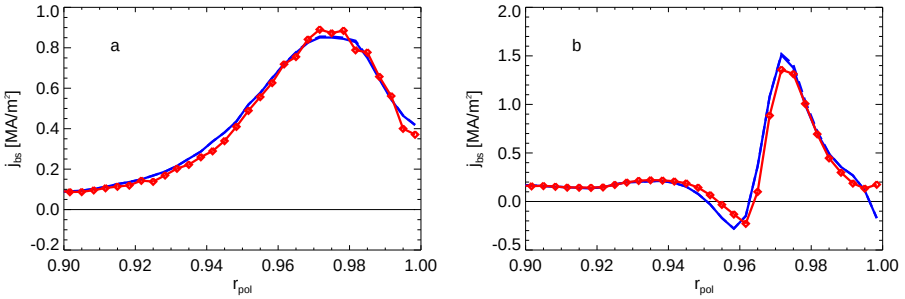

Fig. 8: Bootstrap current (red) in case I (a) and in case II (b). Blue: theory [9].

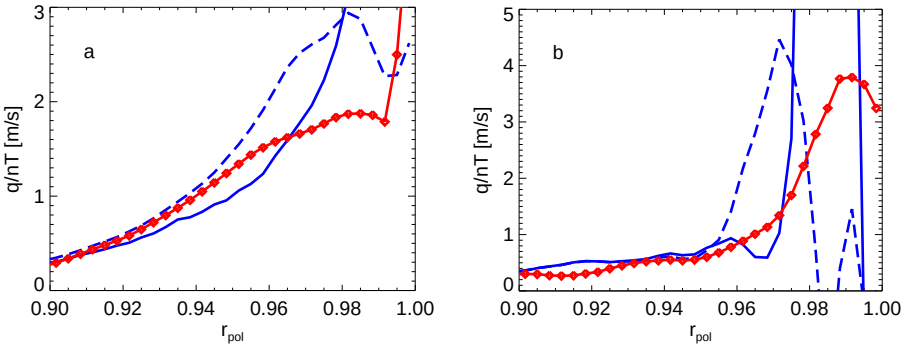

Fig. 9: Heat flux (red) in case I (a) and in case II (b). Blue: theory (solid: [5], dashed: [6]).

across the trapped-passing boundary [6]. but this effect is unlikely to account for the big difference between simulation and the expression from [6] in case II, since $|u/v_{\mathrm{thi}}| < 0.4$ holds up to $r_{\mathrm{pol}} = 0.97$. In Fig. 10 it can be seen that energy scattering (horizontal shift) affects mainly low energy particles at $r_{\mathrm{pol}} = 0.97$ and does even more so at smaller radii, where $|u|$ is smaller. When orbits are widened ($r_{\mathrm{pol}} > 0.98$ in Fig. 9b), the heat flux can be much larger than that of Ref. [6], but is much smaller than that of Ref. [5]. Here, the theory, based on the first two terms in Eq. (1), is not valid, since $\alpha \approx -1$.

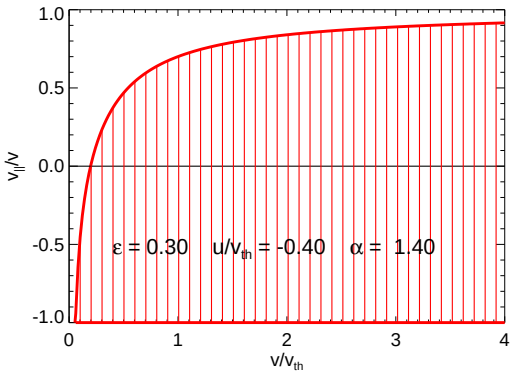

Fig. 10: Region of trapped particles in phase space at $r_{\mathrm{pol}} = 0.97$ in Fig. 9b ($\varepsilon = 0.3$, $u/v_{\mathrm{thi}} = -0.4$, $\alpha = 1.4$).

[1] E. Wolfrum *et al.*, Fus. Energy Conf. IAEA, Geneva 2008, EX/P3-7
[2] F.L. Hinton *et al.*, Rev. Mod. Phys. **48**, 239 (1976)
[3] R.D. Hazeltine, Phys. Fluids **B1**, 2031 (1989)
[4] K.C. Shaing, C.T. Hsu, R.D. Hazeltine, Phys. Plasmas **1**, 3365 (1994)
[5] K.C. Shaing, M.C. Zarnstorff, Phys. Plasmas **4**, 3928 (1997)
[6] G. Kagan, P.J. Catto, Plasma Phys. Contr. Fusion **52**, 055004 (2010)
[7] S.D. Pinches *et al.*, Comp. Phys. Comm. 111, 133 (1998)
[8] A. Bergmann, E. Strumberger and A. G. Peeters, Nucl. Fusion **45**, 1255 (2005)
[9] O. Sauter *et al.*, Phys. Plasmas **6**, 2834 (1999)